graphical plot of K^{-1} *vs.* ϵ (or ΔH°) were not made. The sharpness of fit parameter could also be employed, but the graph has the advantage of showing if a given solution is clearly inconsistent with the others in the set.

Since the equation relating K and ϵ_1 is identical[50] with an equation relating K and ΔH°, this procedure also can be used for calculating enthalpies from calorimetric data.

Acknowledgment.—The authors gratefully acknowledge the support of this research by the National Science Foundation through Grant No. 31431X.

CONTRIBUTION FROM THE INORGANIC CHEMISTRY LABORATORY,
UNIVERSITY OF OXFORD, OXFORD, ENGLAND

The Electronic Spectrum of Trinuclear Chromium(III) Acetate

BY L. DUBICKI AND P. DAY*

Received November 5, 1971

The polarized electronic spectrum of basic chromium(III) acetate, $[Cr_3O(CH_3CO_2)_6(H_2O)_3]Cl\cdot 6H_2O$, is measured over the temperature range 300–4.2°K. The exchange coupling between the three chromium ions is directly observed in the 690–750-nm region where transitions originating from different ground-state spin levels are identified. Tentative assignments of the various transitions are given in terms of excited states constructed from combinations of the ligand-field states defined for the local C_{4v} sites of the individual chromium(III) ions. The intensities of the transitions to excited states derived from $^2A_2$, $^2B_1$, and $^2A_1$ are dominated by the components which originate in the lowest level of the exchange-split $^4B_1$ ground state. A highly structured band system between 365 and 330 nm is assigned to double excitation of the low-energy doublet states.

The optical consequences of exchange interactions between transition metal ions have so far been observed experimentally in two distinct classes of compounds. When such ions are doped at moderate concentrations into diamagnetic host lattices, pairs and other clusters of near-neighbor magnetic ions can occur. The spectra of exchange-coupled pairs of Mn(II) and Ni(II) ions in $KZnF_3$ have been examined by Ferguson, *et al.*[1] At the other extreme, the spectra of pure, magnetically concentrated salts such as MnF_2 have also received a lot of attention recently and have been interpreted in terms of coexcitation of spin-wave packets (magnons) and excitons.[2] From the point of view of the chemist, models of magnetic exchange involving pairs or clusters of ions are conceptually more attractive, but experiments of the type performed by Ferguson encounter the difficulty that many different types of cluster may be present in the lattice at the same time, depending on statistical and energetic considerations. Studies of exchange interactions in discrete polynuclear cluster compounds using bulk susceptibility are well advanced,[3] but no precise single-crystal work appears to have been carried out on their optical spectra. In this paper we report the polarized electronic spectrum of basic chromium(III) acetate at a number of temperatures between 77 and 4°K. This molecule is an attractive one in which to study optical effects of exchange interactions, not only because of its trimeric structure but also because of the light which its spectrum might throw on those of concentrated ruby and pure Cr_2O_3.[4]

The structure of basic chromium(III) acetate, $[Cr_3O(CH_3CO_2)_6(H_2O)_3]Cl\cdot 6H_2O$, has been resolved by X-ray methods.[5,6] The unit cell contains four trimeric units and the space group is $P2_12_12$. The three chromium ions, each pair bridged by two acetate ligands, lie at the apices of an equilateral triangle. The trigonally coordinated oxygen atom in the center of the triangle and the terminal water molecules complete the octahedral coordination at each metal ion (Figure 1).

The three chromium ions are antiferromagnetically coupled.[7-9] Direct Cr–Cr overlap should be very small as the Cr–Cr separation is 3.28 Å. The metal $3d_{xy}$ and $3d_{xz,yz}$ orbitals can overlap with the π orbitals of the acetate ligands, and the $2p\pi$ orbital of the trigonal oxygen atom, respectively. It is likely that the mechanism of the ground-state antiferromagnetism is principally π superexchange. Measurement of the magnetic susceptibility down to 0.5°K yields a Weiss constant of some 0.1°K, indicating that the intercluster interaction is very small.[10]

Kambe[11] has interpreted the magnetic behavior using the spin Hamiltonian $\mathcal{H} = -2J_0[S_1\cdot S_2 + S_3\cdot S_1] - 2(J_0 + J_1)[S_2\cdot S_3]$ where $S_1 = S_2 = S_3 = {}^3/_2$, $J_0 = -15$°K, and $J_1 = -3.25$°K. The use of the J_1 parameter is necessary not only to obtain an improved fit between the calculated and measured magnetic susceptibility but also to ensure that the two lowest Kramers doublet states are split by several wave numbers as demanded by heat capacity measurements.[12,13] How-

(1) J. Ferguson, H. J. Guggenheim, and Y. Tanabe, *J. Phys. Soc. Jap.*, **21**, 692 (1966); *J. Chem. Phys.*, **45**, 1134 (1966).

(2) *E.g.*, D. S. McClure, R. Meltzer, S. A. Reed, P. Russell, and J. W. Stout in "Optical Properties of Ions in Crystals," H. M. Crosswhite and H. W. Moos, Ed., Interscience, New York, N. Y., 1967, p 257; D. D. Sell, R. L. Greene, and R. M. White, *Phys. Rev.*, **158**, 489 (1967).

(3) For a recent review, see R. L. Martin in "New Pathways in Inorganic Chemistry," E. A. V. Ebsworth, A. G. Maddock, and A. G. Sharpe, Ed., Cambridge University Press, London, 1968.

(4) (a) D. S. McClure, *J. Chem. Phys.*, **38**, 2289 (1963); (b) J. W. Allen, R. M. Macfarlane, and R. L. White, *Phys. Rev.*, **179**, 523 (1969).

(5) B. N. Figgis and G. B. Robertson, *Nature (London)*, **205**, 694 (1965).

(6) S. C. Chang and G. A. Jeffrey, *Acta Crystallogr., Sect. B*, **26**, 673 (1970).

(7) A. Welo, *Phys. Rev.*, **32**, 320 (1928).

(8) G. Foëx, B. Tsai, and J. Wucher, *C. R. Acad. Sci.*, **233**, 1432 (1951).

(9) B. Tsai and J. Wucher, *J. Phys. Radium*, **13**, 485 (1952).

(10) J. T. Schriempf and S. A. Friedberg, *J. Chem. Phys.*, **40**, 296 (1964).

(11) K. Kambe, *J. Phys. Soc. Jap.*, **5**, 48 (1950).

(12) J. Wucher and J. D. Wasscher, *Physica*, **20**, 721 (1954).

(13) J. Wucher and H. M. Gijman, *ibid.*, **20**, 361 (1954).

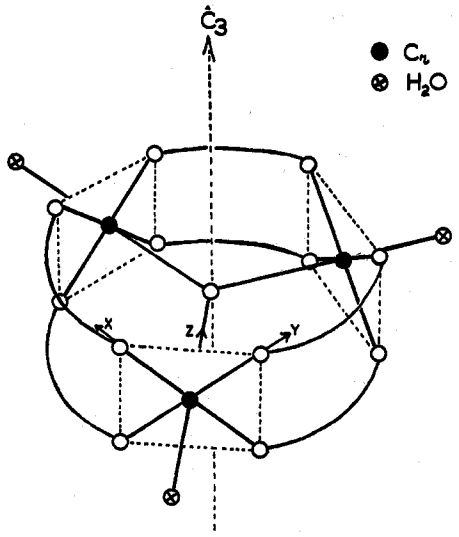

Figure 1.—Schematic drawing of the structure of $[Cr_3O(CH_3CO_2)_6(H_2O)_3]^+$. The local axes at the metal ions are labeled x, y, z. The trimer Z axis is concident with the C_3 axis.

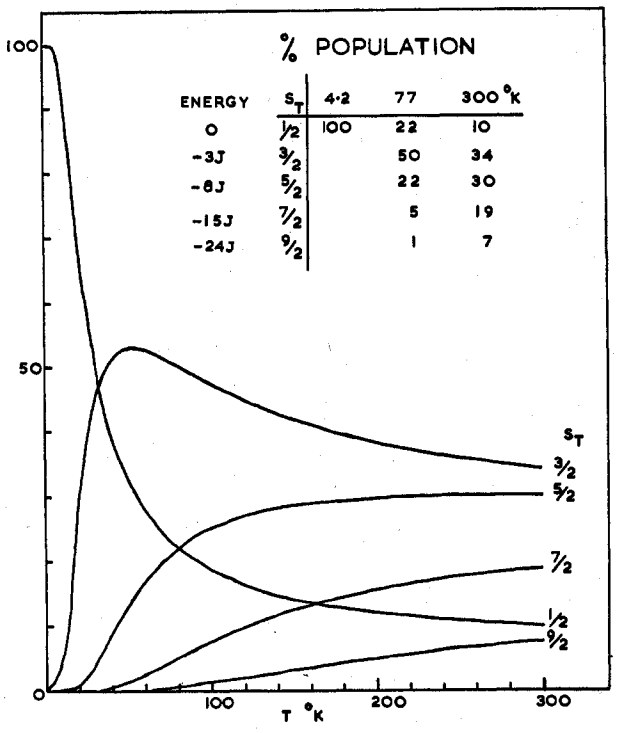

Figure 2.—The temperature dependence of the populations of the ground levels, using $\mathcal{H} = -2J_0[S_1 \cdot S_2 + S_2 \cdot S_3 + S \cdot S_1]$ where $S_1 = S_2 = S_3 = 3/2$, $S_T = S_1 + S_2 + S_3$, and $-J_0 = 15°K$ (10.4 cm^{-1}).

ever, X-ray studies of the cluster at room temperature reveal only small departures from trigonal symmetry. Uryu and Friedberg[14] have suggested that the necessary splitting of the two Kramers doublets can also be achieved by incorporating higher order isotropic terms in the spin Hamiltonian without assuming any distortion of the trinuclear cluster. However, this work has been recently criticized.[15] The temperature dependence of the ground-level populations for $J_0 = -15°K$ and

(14) N. Uryu and S. A. Friedberg, *Phys. Rev. A*, **140**, 1803 (1965).
(15) M. Sorai, M. Tachiki, H. Suga, and S. Seki, *J. Phys. Soc. Jap.*, **30**, 750 (1971).

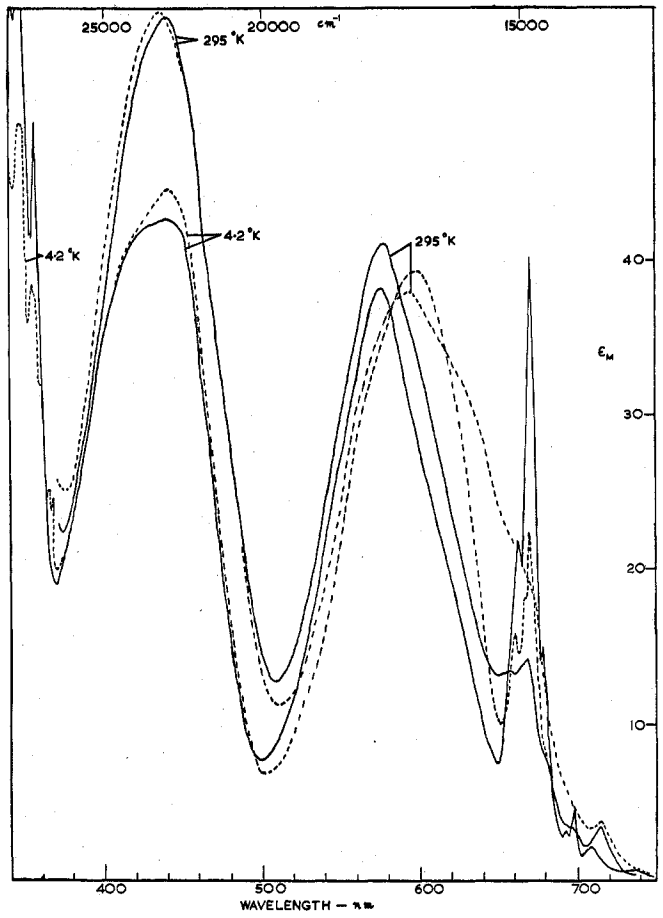

Figure 3.—The electronic spectrum of basic chromium(III) acetate in the visible region. Polarization A is denoted by the full line and polarization B by the broken line. ϵ_M is the molar extinction coefficient per monomer.

$J_1 = 0°K$ is shown in Figure 2. The magnitude of the population changes expected in the temperature range 4–80°K suggest that it should be possible to determine the ground-level origin of the transitions directly by examining the temperature dependence of their intensities. Figure 2 should be adequate for our purpose because transitions from the two lowest Kramers doublets (column (e) of Figure 4) are not resolved, both being appreciably populated at 4.2°K.

The low-resolution spectra of a series of chromium acetate complexes resemble the spectra of single chromium(III) ions in a tetragonal environment.[16] The present higher resolution measurements over the temperature range 300–4.2°K reveal not only the splitting of the ground-state manifold but also the intracluster Davydov splitting of the excited states. In the discussion of the electronic spectrum we assume that the point group of the cluster is D_{3h}.

Experimental Section

The slow evaporation of aqueous solutions of $[Cr_3O(CH_3CO_2)_6(H_2O)_3]Cl \cdot 6H_2O$ usually produced two types of crystals, thin plates and prisms of pseudohexagonal symmetry. The former were strongly dichroic and the reported spectra were obtained from the thin plates. For the prisms, the spectra along the two extinction directions were similar and nearly identical with the spectrum along one of the extinction directions, B, of the thin plates. An X-ray study of the latter showed that the well-

(16) L. Dubicki and R. L. Martin, *Aust. J. Chem.*, **22**, 701 (1969).

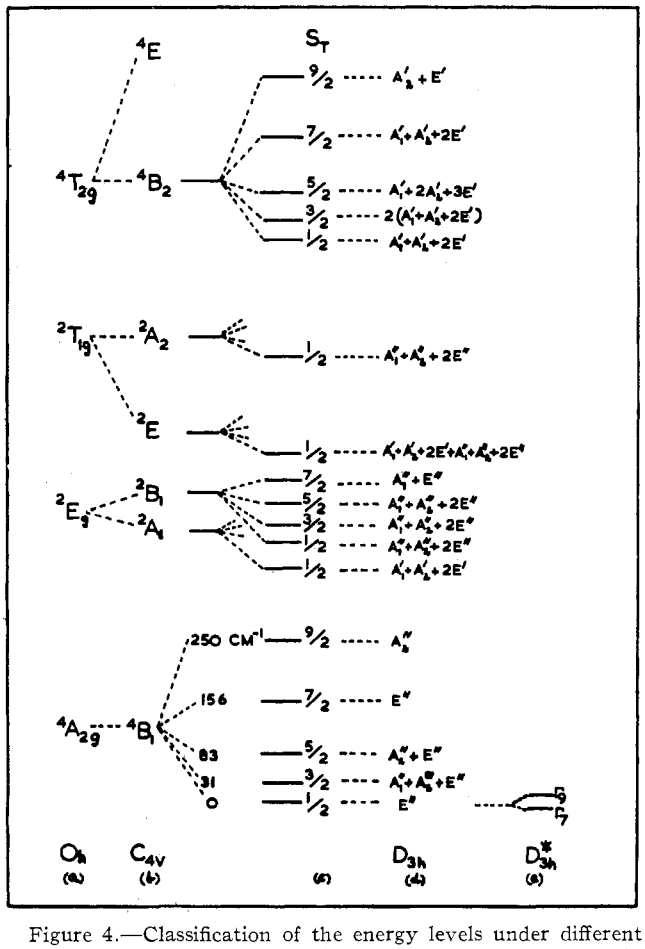

Figure 4.—Classification of the energy levels under different types of perturbation. (a) and (b) show the ligand field states in O_h and C_{4v} microsymmetry, respectively. (c) shows the exchange splitting of the ligand field states into states characterized by the total spin quantum number $S_T = S_1 + S_2 + S_3$. The ordering of the excited states is arbitrary. (d) shows the symmetry species of the trimer wave functions which are eigenfunctions of S_T and which are antisymmetric with respect to electron exchange between the metal ions. The spin multiplicity $(2S_T + 1)$ of the trimer stakes is omitted. (e) shows the inclusion of spin–orbit coupling.

developed face was (110). The direction cosines of the extinction directions, A and B, with respect to the crystallographic axes a, b, c are 0.0, 0.0, 1.0 for A and −0.509, +0.861, 0.0 for B. The direction cosines of the unit vector along the C_3 axis (Z) of the cluster with respect to a, b, c are for the four trimeric units ±0.7219, ±0.6623, +0.2005, and ±0.7219, ±0.6623, +0.2005. The intensities along the crystal extinction directions are related to the intensities along the cluster Z and XY axes by

$$E_A = 0.04E_Z + 0.96E_{XY}$$

$$E_B = 0.46E_Z + 0.54E_{XY}$$

The spectra were recorded on a Cary 14 spectrophotometer. Polarized spectra were obtained by placing a Glan prism before the sample. Crystals were mounted over a hole in a copper sheet which was fixed to the base of the liquid helium container of an Oxford Instruments cryostat. The very slow rate of warming of the cryostat permitted the measurement of the spectra as a function of temperature, using a gold–0.03 atom % iron *vs.* chromel thermocouple. Since the complex contains water of crystallization, it was necessary to lower the temperature before gently reducing the pressure.

Results and Discussion

The Spin-Allowed Ligand Field Bands.—The general features of the visible spectrum (Figure 3 and Table I) resemble those of chromium(III) ions in near-octahedral fields,[17] with the broad absorptions at 590 and 440 nm corresponding to the $^4A_{2g} \rightarrow {}^4T_{2g}$ and $^4A_2 \rightarrow {}^4T_{1g}$ transitions. In addition to these two broad bands, there is another, much sharper band system near 670 nm, whose intensity might at first sight suggest an assignment as a low-symmetry component of $^4T_{2g}$. Indeed, in an earlier paper[16] such an assignment was shown to be compatible with a small positive value of Dt. This region of the spectrum bears a striking similarity to the corresponding part of the Cr_2O_3 spectrum and for this, as well as for a number of other reasons detailed in the following section, we now prefer to regard the sharp band system at 670 nm as a component of the doublet spectrum, despite its apparently high intensity. In this connection, it should be pointed out that although the 670-nm band has a maximum extinction coefficient almost equal to those of the bands assigned to $^4T_{1g}$ and $^4T_{2g}$, its half-width is nearly an order of magnitude smaller.

TABLE I
SPECTRAL DATA IN THE VISIBLE REGION AT 4.2°K

Band[a]	Obsd freq, cm^{-1} Polarizn A^b	Obsd freq, cm^{-1} Polarizn B^b	Assignment
1	14,735		
2	14,900	14,900	
3	14,990 sh	14,995	$^2A_2(^2T_{1g})$
4	15,095		
5		15,120	
	17,390	16,670	$^4B_1$, $^4E(^4T_{2g})$
	22,600	22,600	^4E, $^4A_2(^4T_{1g})$
	23,800 sh	23,800 sh	

[a] See Figure 5. [b] See text for definitions.

The $^4T_{2g}$ band at 590 nm is split into two components with maxima at 16,670 and 17,390 cm^{-1} which are polarized along the Z and XY axes of the trimer, respectively. This splitting is probably due to the local tetragonal field, and the excited states are assigned as $^4B_2$(16,670 cm^{-1}) and ^4E(17,390 cm^{-1}). The $^4T_{1g}$ band at 440 nm does not show any large splitting, indicating that κ ($=Ds/Dt$) is small. Since the $^4A_2(^4T_{1g})$ component is not resolved, it is not possible to determine the sign of κ.

The exchange interaction between the chromium ions can provide an exchange-induced dipole moment mechanism[18] for the intensification of electronic transitions. Neglecting spin–orbit coupling, the selection rule for spin is $\Delta S_T = 0$ and $\Delta M_T = 0$, where S_T is the total spin quantum number for the trimer. The orbital selection rules are derived by determining the transformation properties of the eigenfunctions of S_T under the symmetry operations of the D_{3h} point group. The eigenfunctions of S_T are listed in the Appendix and the representations of the resulting states are given in column (d) of Figure 4. Using Table II and extending Figure 4 to the spin-allowed transitions it can be shown that $^4B_1 \rightarrow {}^4E$ transitions are allowed in XY and Z polarization while $^4B_1 \rightarrow {}^4B_2$ and $^4B_1 \rightarrow {}^4A_2$ are allowed in Z and XY polarization, respectively. The $^4B_1 \rightarrow {}^4E$ transitions are xy allowed in local C_{4v} symmetry so that it is not possible on the basis of the polarization data to discriminate between single-ion and exchange-induced dipole moment mechanism. At the same time our as-

(17) J. R. Perumareddi, *J. Phys. Chem.*, **71**, 3144, 3155 (1967).
(18) Y. Tanabe, T. Moriya, and S. Sugano, *Phys. Rev. Lett.*, **15**, 1023 (1965).

TABLE II
ELECTRIC DIPOLE SELECTION RULES IN D_{3h} AND IN THE DOUBLE GROUP D_{3h}*

		A_1'	A_2'	A_1''	A_2''	E''	E'			
		Γ_1	Γ_2	Γ_3	Γ_4	Γ_5	Γ_6	Γ_7	Γ_8	Γ_9
A_1'	Γ_1				z		xy			
A_2'	Γ_2			z			xy			
A_1''	Γ_3		z			xy				
A_2'	Γ_4	z				xy				
E''	Γ_5			xy	xy	xy	z			
E'	Γ_6	xy	xy			z	xy			
	Γ_7								xyz	xy
	Γ_8							xyz		xy
	Γ_9							xy	xy	z

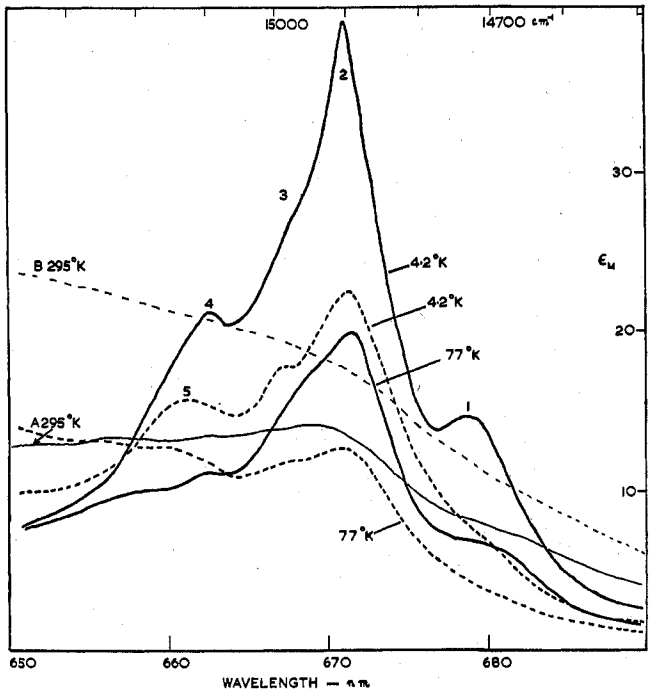

Figure 5.—The 670-nm absorption in basic chromium(III) acetate. Polarization A is denoted by the full line and polarization B by the broken line. ϵ_M is the molar extinction coefficient per monomer.

signment of the 16670-cm^{-1} band to $^4B_1 \rightarrow {}^4B_2$ is consistent with the selection rules for a cooperative mechanism. The intensities of $^4E(^4T_{2g})$ and $^4T_{1g}$ decrease by some 17 and 30%, respectively, as the temperature is lowered from 295 to 4.2°K, indicating that they are at least partly phonon assisted.

The 670-Nm Absorption.—The 650–690-nm absorption (Figure 5 and Table I) has an effective band width of about 250 cm^{-1} while the two components of $^4T_{2g}$ in A and B polarizations have bandwidths of 2100 and 2400 cm^{-1}, respectively. The remarkably small width of the 670-nm band is strong evidence for rejecting the assignment $^4B_1 \rightarrow {}^4B_2$. The latter corresponds to a one-electron excitation into a strongly antibonding orbital, $(xz)^1(yz)^1(xy)^1 \rightarrow (xz)^1(yz)^1(x^2 - y^2)^1$.[17]

In A polarization the intensity of the 650–690-nm absorption decreases by a factor of 2.1 in the range 4.2–77°K. According to Figure 2 the population of the $S = {}^1/_2$ ground level decreases by a factor of 4.5. Hence transitions from $S = {}^1/_2$ and other ground levels must be contributing to the absorption but the $S = {}^1/_2$ transitions are more intense by at least a factor of 2. The fine structure, labeled as bands 1–5 in Figure 5, does not change in position by more than 10 cm^{-1} yet the ground-level energies are 0, 31, 83, 156 cm^{-1} for $S = {}^1/_2, {}^3/_2, {}^5/_2, {}^7/_2$, respectively. Apparently the splitting of the excited states with different S values is similar to the ground-state splitting. Furthermore the spin-selection rule may be $\Delta S_T = 0$ since transitions originating from different ground levels do not terminate in the same excited state. According to Figure 4 and Table II the $^4B_1 \rightarrow {}^2A_2(^2T_{1g})$ and $^4B_1 \rightarrow {}^2E(^2T_{1g})$ transitions should be XY and XYZ polarized, respectively. The predominantly XY-polarized 650–690-nm absorption is therefore assigned as $^4B_1 \rightarrow {}^2A_2$, though it is not clear whether the fine structure consists of phonon side bands or intracluster Davydov components.

If the 670-nm absorption is assigned as $^4B_1 \rightarrow {}^2A_2(^2T_{1g})$, it is clear that the corresponding band in Cr_2O_3 is also intensified, in contrast to the acid erythro salt $[(NH_3)_5Cr(OH)Cr(NH_3)_4(H_2O)]Cl_5 \cdot H_2O$,[19] in which it remains relatively weak. This suggests a correlation with the Cr–O–Cr angle, which is 82° in Cr_2O_3[4a] and 120° in trinuclear chromium(III) acetate but approaches 180° in the acid erythro salt. One possible explanation for these observations is that for a pair (a, b) of chromium(III) ions an orbital change and spin flip of the type $x^+z_a \rightarrow y^-z_a$ (which corresponds to the transition $^4B_1 \rightarrow {}^2A_2$ in C_{4v} microsymmetry) may be relatively intense if the $3d_{xz_a}$ and $3d_{yz_b}$ orbitals can overlap either directly or, perhaps more significantly, *via* bridging ligand orbitals, as is the case in chromium(III) acetate. For a linear CrOCr group with D_{4h} symmetry the spin-flip transition $x^+z_a \rightarrow x^-z_a$ ($^4B_1 \rightarrow {}^2A_1, {}^2B_1$) is more intense because $3d_{xz_a}$ overlaps with $3d_{xz_b}$ but is orthogonal to $3d_{yz_b}$.

The Low-Energy Quartet–Doublet Absorption.—The 690–750-nm absorption contains transitions corresponding to $^4A_{2g} \rightarrow {}^2E_g, {}^2T_{1g}$ in octahedral chromium(III) complexes. The spectra are shown in Figures 6 and 7 and the band energies are listed in Table III.

TABLE III
PEAK MAXIMA (CM^{-1}) IN THE 690–750-NM REGION

Band[a]	A(4.2°K)[b]	B(4.2°K)[c]	A(77°K)	B(77°K)	Ground-state origin, S_T
1	13,369	13,369 XY			
2	13,445	13,445 XY			
3	13,490	13,485 Z			$^1/_2$
4	13,510				
5	13,550	13,535 Z			
6	13,600	13,600 Z			
7	13,660	13,640 Z			
8	13,735				
9	13,795				
10	13,865				
11			13,890	13,900 Z	$^5/_2$
12			14,015	14,040 Z	$^3/_2$
13	14,080	14,110 Z			$^1/_2$
14		14,210 Z	14,205	14,205 Z	$^1/_2$, $^3/_2$, $^5/_2$
15	14,330	14,330 XY	14,330	14,330 XY	$^1/_2$, $^3/_2$
16	14,440	14,460 Z	14,440	14,460 Z	$^1/_2$

[a] Refer to Figures 6 and 7. [b] All bands appearing in the A spectrum are XY polarized. [c] Polarizations deduced from dichroic ratios and peak positions.

It is difficult to measure the intensities and dichroic ratios accurately because of overlap between the bands and the temperature-dependent contribution from the $^4B_1 \rightarrow {}^2A_2$ absorption. However the assignment of the band polarizations is generally in qualitative agreement

(19) L. Dubicki, *Aust. J. Chem.*, in press.

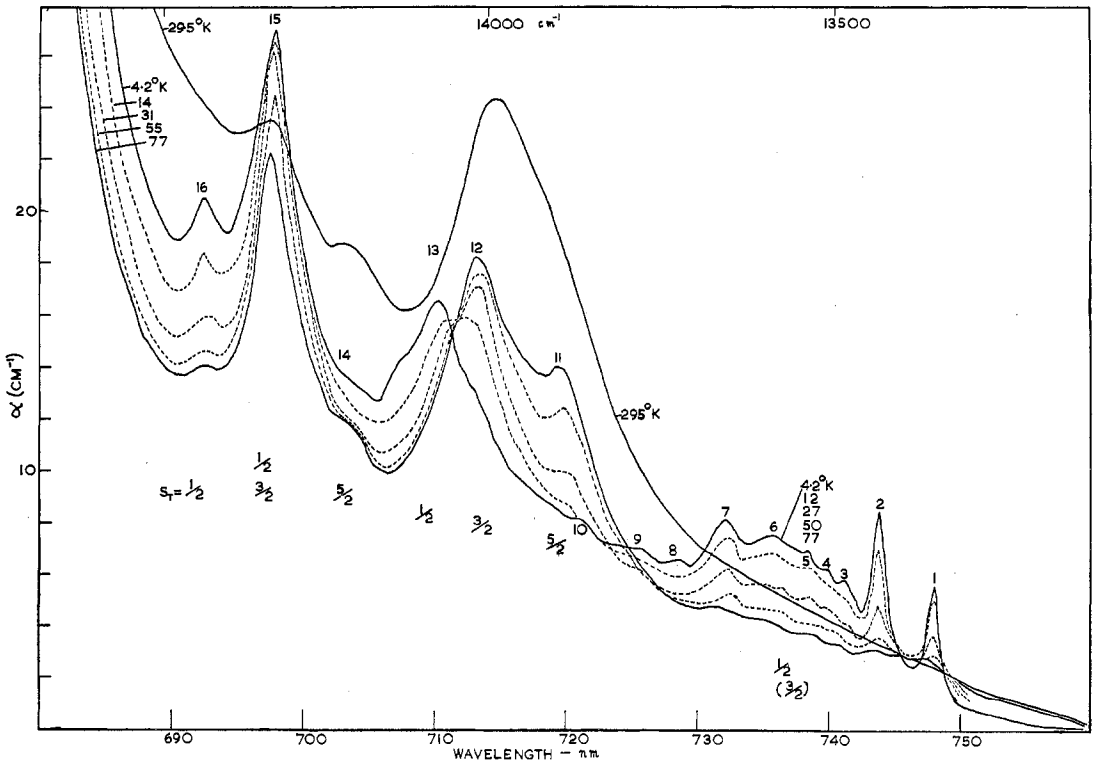

Figure 6.—The low-energy quartet–doublet absorption of basic chromium acetate in A polarization. α is defined as optical density per thickness (cm). To convert α into the molar extinction coefficient per monomer, multiply by 0.145.

with the predicted dichroic ratios; *viz.*, for an XY-polarized band E_B/E_A is roughly 0.5 and for a Z-polarized band E_B/E_A is large.

The absorption in the 690–750-nm region appears to consist of three band systems, the first of which we take as extending from 690 to 705 nm. From the temperature dependence of the intensities it is possible, by making use of Figure 2, to determine the ground-state origins of most of the bands. Thus the ground-state origin of band 16 is assigned as $S = {}^1/_2$ since the intensity is reduced by a factor of about 4 in the range 4.2–77°K. On the other hand the intensity of band 15 passes through a maximum between 30 and 77°K, so transitions from both $S = {}^1/_2$ and ${}^3/_2$ must contribute. The peak position of this band does not change so that the $S = {}^1/_2$ and ${}^3/_2$ transitions terminate in excited states which have the same separation as the two ground levels, *viz.*, $-3J_0 \approx 31$ cm^{-1}. Band 15 is more intense in A polarization roughly by a factor of 2 and is therefore XY polarized. The temperature dependence of the Z-polarized component of band 14 is similar to band 15. In contrast, the intensity of the XY-polarized component of band 14, which is scarcely seen at 4.2°K, continues to increase above 77°K, so that it must originate from $S = {}^5/_2$.

The second band system (710–725 nm) provides a particularly clear illustration of the ground manifold of levels, since it consists of two sets of three bands, whose members originate from different components of the ground state. In the A spectrum, as the temperature increases from 4.2°K, band 13 rapidly decreases in intensity while band 12 rapidly increases. The intensity of the latter reaches a maximum between 50 and 77°K. In addition, band 11 increases rather slowly in intensity with increasing temperature. These observations are easily interpreted by assigning the ground-state origins of bands 11–13 as $S_T = {}^5/_2$, ${}^3/_2$, and ${}^1/_2$, respectively. The spin-selection rule $\Delta S_T = 0$ appears to operate, although the separations between the excited states with $S_T = {}^1/_2$, ${}^3/_2$, and ${}^5/_2$ do not follow those predicted from a total-spin Heisenberg-exchange Hamiltonian. However, it is now recognized[4b] that in general such a Hamiltonian, representing isotropic exchange, is not an adequate representation of the interaction between ions in states of differing total spin. It is noticeable that in B polarization the corresponding three bands lie at different energies to the A-polarized bands. This indicates that for each value of S_T there are two excited states, one giving rise to XY- and the other to Z-polarized transitions.

The third band system (725–750 nm) contains both Z- and XY-polarized absorption. In A polarization the intensities of all the bands 1–7 are reduced by a factor of about 4 on increasing the temperature from 4.2 to 77°K. In B polarization the corresponding reduction is nearer twofold, although the difference may be accounted for by the error in choosing the base line. The temperature dependence thus demonstrates quite clearly that, as for the ${}^4B_1 \rightarrow {}^2A_2$ absorption region, transitions from the $S_T = {}^1/_2$ ground level dominate the entire group of bands. The fine structure of bands 1–7 thus remains unassigned. If it is not the result of vibrational coexcitations (and there is no sign of any similar structure attached to the higher energy doublet transitions), then it must be attributed to an intramolecular Davydov effect.

We may tentatively assign the three band systems by reference to Figure 4. The parent octahedral ${}^2T_{1g}$ and ${}^2E_g$ states are split, in the C_{4v} local symmetry of complex, into ${}^2A_2 + {}^2E$ and ${}^2B_1 + {}^2A_1$. The highest

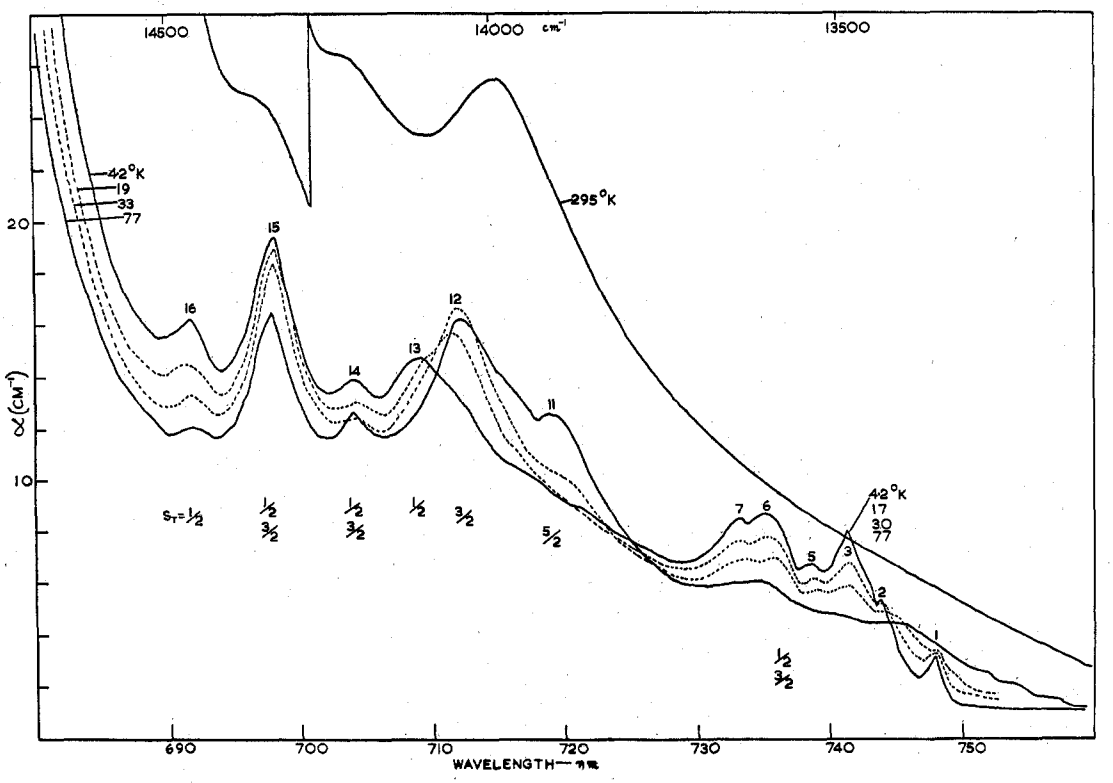

Figure 7.—The low-energy quartet–doublet absorption of basic chromium acetate in B polarization. The definition of α is the same as in Figure 6.

energy system (bands 14–16 in Figures 6 and 7) is then ascribed, with bands 1–5 of Figure 5, to cluster states arising from $^2A_2$ and the next (bands 11–13) to states arising from ^2E. Bands 1 and 2 and their accompanying fine structure then result from $^2A_1$ and $^2B_1$. These conclusions agree quite well with the polarization selection rules derived from the symmetry-adapted combinations of local wave functions, which are given in the Appendix and which lead to the cluster-state labels shown in column (d) of Figure 4. The exchange-induced dipole moment mechanism therefore dominates for these spin-forbidden bands. For example, $^4B_1 \rightarrow {}^2B_1$ is allowed in XY polarization (band 1) and $^4B_1 \rightarrow {}^2A_1$ in Z (band 3). Likewise the components of $^4B_1 \rightarrow {}^2E$, assigned as bands 11–13, are allowed in XY and Z according to Figure 4. Finally band 15 is indeed predominantly XY polarized, as required of a component of $^4B_1 \rightarrow {}^2A_2$, though the Z-polarized intensity of bands 14 and 16 is not explained.

The Near-Ultraviolet Spectrum.—As can be seen in outline from Figure 3, a further set of relatively sharp absorption bands is found in the ultraviolet region, to higher energy than the main quartet absorption. The 4.2°K spectrum of this region is shown in greater detail in Figure 8, and the peak maxima are listed in Table IV. The crystal spectrum is very much better resolved than the 77°K diffuse-reflectance spectrum previously reported.

We do not consider that this structured absorption represents the onset of the second $^4T_{1g}$ transition, partly because we would expect the energy of that transition to be 2000–3000 cm^{-1} higher and partly because, by comparison with complexes in which it has been resolved, we would not expect it to show so much fine structure. The most plausible assignment of the bands

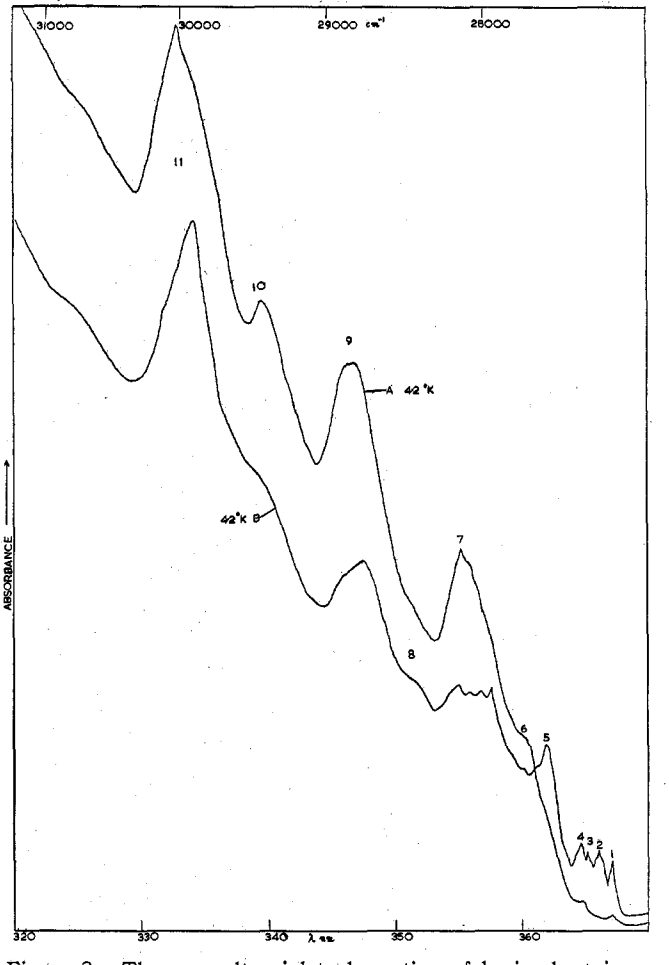

Figure 8.—The near-ultraviolet absorption of basic chromium(III) acetate in A and B polarizations.

TABLE IV
PEAK MAXIMA (cm^{-1}) IN THE NEAR-ULTRAVIOLET REGION, AT 4.2°K

Band	Polarizn *A*	Polarizn *B*	Band	Polarizn *A*	Polarizn *B*
11	30,055	29,965	6	27,760	
10	29,480	29,480	5		27,635
9	28,885	28,800	4	27,435	27,435
8		28,470	3		27,390
7	28,150	28,190	2		27,335
		27,995	1	27,253	27,255

is to simultaneous double excitations of the $^4A_{2g} \rightarrow {}^2E_g$, $^2T_{1g}$ transitions, made allowed by the exchange interaction. Such transitions are well authenticated in the spectra of concentrated ruby crystals, where they occur in the 340-nm region, and in the present case their energies agree quite well with expectation. Thus bands 1–5 in Figure 8 may correspond to the double $^4A_{2g} \rightarrow {}^2E_g$ transitions. Extending the energy level diagram of Figure 4 to doubly excited states, it can be shown that "symmetric" double excitations of the type $^4B_1$, $^4B_1$, $^4B_1 \rightarrow {}^4B_1$, $^2A_1$, $^2A_1$ and $^4B_1$, $^2B_1$, $^2B_1$ are allowed in XY polarization while the "asymmetric" ones $^4B_1$, $^4B_1$, $^4B_1 \rightarrow {}^4B_1$, $^2A_1$, $^2B_1$ are allowed in Z. At first sight the higher energy bands, between 355 and 330 nm, appear to constitute a vibronic progression, but a closer examination of the frequency intervals (Table IV) shows that they are too irregular to make such an interpretation plausible.

Conclusions

As expected, the gross features of the spectrum of trinuclear chromium(III) acetate may be interpreted as due to tetragonally distorted chromium(III), but much of the fine structure, particularly in the 690–750-nm region, is a direct consequence of the exchange coupling within the trimer. From the temperature dependence of the intensities, the ground-state origins of many of the doublet absorption bands can definitely be identified, though some features of the excited-state fine structure remain obscure. For example, it is not clear whether bands 3–7 in Figures 6 and 7 have their origin in vibrational or Davydov interactions.

Perhaps the most unusual feature of the low-energy doublet region is the way in which the absorption which we have assigned to the states arising from $^2A_1$, $^2A_2$, and $^2B_1$ comes, in its entirety, from molecules in the $S_T = {}^1/_2$ component of the ground state, while the band system ^2E contains quite appreciable contributions from $S_T = {}^3/_2$ and ${}^5/_2$. It seems that a selection rule is operating, whose origin remains obscure to us at the present time. From a pure symmetry point of view there appears to be no reason why transitions such as $^4B_1(S_T = {}^3/_2) \rightarrow {}^2A_1(S_T = {}^3/_2)$ should not be allowed. Similar remarks apply to the $^4B_1 \rightarrow {}^2A_2$ region. It is clear that a completely unambiguous band-by-band analysis of this interesting spectrum will require a quantitative application of the theory of exchange interactions to spin-flop and orbital-change transitions.

Acknowledgment.—We are grateful to the Royal Commission for the Exhibition of 1851 for a Research Scholarship (to L. D.) and to the Science Research Council for an equipment grant. We are also indebted to Professor D. S. McClure for an illuminating discussion about the spectrum of Cr_2O_3.

Appendix

The eigenfunctions $\psi(S_T, M_T)$ of the total spin angular momentum, $S = S_1 + S_2 + S_3$, can be obtained as linear combinations of the product functions (S_1M_1, S_2M_2, S_3M_3) using Wigner's 3-j symbols.[20] M_i are the z components of S_i and the product functions are taken to be normalized Slater determinants. The eigenfunctions for $S_1 = S_2 = {}^1/_2$ and $S_3 = {}^1/_2$ are given below. Only positive values of M_T are considered and the S_i symbols are omitted. The eigenfunctions for $S_1 = {}^3/_2$, $S_2 = {}^3/_2$, $S_2 = {}^1/_2$; $S_1 = {}^3/_2$, $S_2 = {}^1/_2$, $S_3 = {}^3/_2$; and $S_1 = {}^1/_2$, $S_2 = {}^3/_2$, $S_3 = {}^3/_2$ form bases for representations of the D_{3h} point group and are applicable to the singly excited ^2E_g, $^2T_{1g}$ states in trinuclear chromium(III) acetate. The eigenfunctions for $S_1 = S_2 = S_3 = {}^3/_2$ have been published by Uryu and Friedberg.[14]

$$S_{12} = S_1 + S_2, \quad S_1 = S_2 = \frac{3}{2}$$

$$S = S_{12} + S_3, \quad S_3 = \frac{1}{2}$$

$S_T = \frac{7}{2}$, $S_{12} = \frac{6}{2}$:

$$\psi\left(\frac{7}{2}, \frac{7}{2}\right) = \left(+\frac{3}{2}, +\frac{3}{2}, +\frac{1}{2}\right)$$

$$\psi\left(\frac{7}{2}, \frac{5}{2}\right) = \frac{1}{\sqrt{7}}\left\{\left(+\frac{3}{2}, +\frac{3}{2}, -\frac{1}{2}\right) + \sqrt{3}\left[\left(+\frac{3}{2}, +\frac{1}{2}, +\frac{1}{2}\right) + \left(+\frac{1}{2}, +\frac{3}{2}, +\frac{1}{2}\right)\right]\right\}$$

$$\psi\left(\frac{7}{2}, \frac{3}{2}\right) = \frac{1}{\sqrt{7}}\left\{\left(+\frac{3}{2}, +\frac{1}{2}, -\frac{1}{2}\right) + \left(+\frac{1}{2}, +\frac{3}{2}, -\frac{1}{2}\right) + \left(+\frac{3}{2}, -\frac{1}{2}, +\frac{1}{2}\right) + \left(-\frac{1}{2}, +\frac{3}{2}, +\frac{1}{2}\right) + \sqrt{3}\left(+\frac{1}{2}, +\frac{1}{2}, +\frac{1}{2}\right)\right\}$$

$$\psi\left(\frac{7}{2}, \frac{1}{2}\right) = \frac{1}{\sqrt{35}}\left\{\sqrt{3}\left[\left(+\frac{3}{2}, -\frac{1}{2}, -\frac{1}{2}\right) + \left(-\frac{1}{2}, +\frac{3}{2}, -\frac{1}{2}\right)\right] + 3\left[\left(+\frac{1}{2}, +\frac{1}{2}, -\frac{1}{2}\right) + \left(+\frac{1}{2}, -\frac{1}{2}, +\frac{1}{2}\right) + \left(-\frac{1}{2}, +\frac{1}{2}, +\frac{1}{2}\right)\right] + \left(+\frac{3}{2}, -\frac{3}{2}, +\frac{1}{2}\right) + \left(-\frac{3}{2}, +\frac{3}{2}, +\frac{1}{2}\right)\right\}$$

$S_T = \frac{5}{2}$, $S_{12} = \frac{6}{2}$:

$$\psi\left(\frac{5}{2}, \frac{5}{2}\right) = \frac{1}{\sqrt{14}}\left\{2\sqrt{3}\left(+\frac{3}{2}, +\frac{3}{2}, -\frac{1}{2}\right) - \left(+\frac{3}{2}, +\frac{1}{2}, +\frac{1}{2}\right) - \left(+\frac{1}{2}, +\frac{3}{2}, +\frac{1}{2}\right)\right\}$$

(20) M. Rotenberg, R. Bivins, N. Metropolis, and J. K. Wooten, Jr., "The 3-j and 6-j Symbols," Technology Press, Massachusetts Institute of Technology, Cambridge, Mass., 1959.

$$\psi\left(\frac{5}{2}, \frac{3}{2}\right) = \frac{1}{\sqrt{70}}\left\{5\left[\left(+\frac{3}{2}, +\frac{1}{2}, -\frac{1}{2}\right) + \left(+\frac{1}{2}, +\frac{3}{2}, -\frac{1}{2}\right)\right] - 2\left[\left(+\frac{3}{2}, -\frac{1}{2}, +\frac{1}{2}\right) + \left(-\frac{1}{2}, +\frac{3}{2}, +\frac{1}{2}\right) + \sqrt{3}\left(+\frac{1}{2}, +\frac{1}{2}, +\frac{1}{2}\right)\right]\right\}$$

$$\psi\left(\frac{5}{2}, \frac{1}{2}\right) = \frac{1}{2\sqrt{35}}\left\{4\left[\left(+\frac{3}{2}, -\frac{1}{2}, -\frac{1}{2}\right) + \left(-\frac{1}{2}, +\frac{3}{2}, -\frac{1}{2}\right) + \sqrt{3}\left(+\frac{1}{2}, +\frac{1}{2}, -\frac{1}{2}\right)\right] - \sqrt{3}\left[\left(+\frac{3}{2}, -\frac{3}{2}, +\frac{1}{2}\right) + \left(-\frac{3}{2}, +\frac{3}{2}, +\frac{1}{2}\right) + 3\left(+\frac{1}{2}, -\frac{1}{2}, -\frac{1}{2}\right) + 3\left(-\frac{1}{2}, +\frac{1}{2}, +\frac{1}{2}\right)\right]\right\}$$

$S_T = \frac{5}{2}$, $S_{12} = \frac{4}{2}$:

$$\psi\left(\frac{5}{2}, \frac{5}{2}\right) = \frac{1}{\sqrt{2}}\left\{\left(+\frac{3}{2}, +\frac{1}{2}, +\frac{1}{2}\right) - \left(+\frac{1}{2}, +\frac{3}{2}, +\frac{1}{2}\right)\right\}$$

$$\psi\left(\frac{5}{2}, \frac{3}{2}\right) = \frac{1}{\sqrt{10}}\left\{\left(+\frac{3}{2}, +\frac{1}{2}, -\frac{1}{2}\right) - \left(+\frac{1}{2}, +\frac{3}{2}, -\frac{1}{2}\right) + 2\left(+\frac{3}{2}, -\frac{1}{2}, +\frac{1}{2}\right) - 2\left(-\frac{1}{2}, +\frac{3}{2}, +\frac{1}{2}\right)\right\}$$

$$\psi\left(\frac{5}{2}, \frac{1}{2}\right) = \frac{1}{2\sqrt{5}}\left\{2\left[\left(+\frac{3}{2}, -\frac{1}{2}, -\frac{1}{2}\right) - \left(-\frac{1}{2}, +\frac{3}{2}, -\frac{1}{2}\right)\right] + \sqrt{3}\left[\left(+\frac{3}{2}, -\frac{3}{2}, +\frac{1}{2}\right) - \left(-\frac{3}{2}, +\frac{3}{2}, +\frac{1}{2}\right) + \left(+\frac{1}{2}, -\frac{1}{2}, +\frac{1}{2}\right) - \left(-\frac{1}{2}, +\frac{1}{2}, +\frac{1}{2}\right)\right]\right\}$$

$S_T = \frac{3}{2}$, $S_{12} = \frac{4}{2}$:

$$\psi\left(\frac{3}{2}, \frac{3}{2}\right) = \frac{1}{\sqrt{10}}\left\{2\left[\left(+\frac{3}{2}, +\frac{1}{2}, -\frac{1}{2}\right) - \left(+\frac{1}{2}, +\frac{3}{2}, -\frac{1}{2}\right)\right] - \left(+\frac{3}{2}, -\frac{1}{2}, +\frac{1}{2}\right) + \left(-\frac{1}{2}, +\frac{3}{2}, +\frac{1}{2}\right)\right\}$$

$$\psi\left(\frac{3}{2}, \frac{1}{2}\right) = \frac{1}{2\sqrt{5}}\left\{\sqrt{6}\left[\left(+\frac{3}{2}, -\frac{1}{2}, -\frac{1}{2}\right) - \left(-\frac{1}{2}, +\frac{3}{2}, -\frac{1}{2}\right)\right] - \sqrt{2}\left[\left(+\frac{3}{2}, -\frac{3}{2}, +\frac{1}{2}\right) - \left(-\frac{3}{2}, +\frac{3}{2}, +\frac{1}{2}\right) + \left(+\frac{1}{2}, -\frac{1}{2}, +\frac{1}{2}\right) - \left(-\frac{1}{2}, +\frac{1}{2}, +\frac{1}{2}\right)\right]\right\}$$

$S_T = \frac{3}{2}$, $S_{12} = \frac{2}{2}$:

$$\psi\left(\frac{3}{2}, \frac{3}{2}\right) = \frac{1}{\sqrt{10}}\left\{\sqrt{3}\left[\left(+\frac{3}{2}, -\frac{1}{2}, +\frac{1}{2}\right) + \left(-\frac{1}{2}, +\frac{3}{2}, +\frac{1}{2}\right)\right] - 2\left(+\frac{1}{2}, +\frac{1}{2}, +\frac{1}{2}\right)\right\}$$

$$\psi\left(\frac{3}{2}, \frac{1}{2}\right) = \frac{1}{\sqrt{30}}\left\{\sqrt{3}\left(+\frac{3}{2}, -\frac{1}{2}, -\frac{1}{2}\right) + \sqrt{3}\left(-\frac{1}{2}, +\frac{3}{2}, -\frac{1}{2}\right) - 2\left(+\frac{1}{2}, +\frac{1}{2}, -\frac{1}{2}\right) + 3\left(+\frac{3}{2}, -\frac{3}{2}, +\frac{1}{2}\right) + 3\left(-\frac{3}{2}, +\frac{3}{2}, +\frac{1}{2}\right) - \left(+\frac{1}{2}, -\frac{1}{2}, +\frac{1}{2}\right) - \left(-\frac{1}{2}, +\frac{1}{2}, +\frac{1}{2}\right)\right\}$$

$S_T = \frac{1}{2}$, $S_{12} = \frac{2}{2}$:

$$\psi\left(\frac{1}{2}, \frac{1}{2}\right) = \frac{1}{2\sqrt{15}}\left\{2\left[\sqrt{3}\left(+\frac{3}{2}, -\frac{1}{2}, -\frac{1}{2}\right) + \sqrt{3}\left(-\frac{1}{2}, +\frac{3}{2}, -\frac{1}{2}\right) - 2\left(+\frac{1}{2}, +\frac{1}{2}, -\frac{1}{2}\right)\right] - 3\left(+\frac{3}{2}, -\frac{3}{2}, +\frac{1}{2}\right) - 3\left(-\frac{3}{2}, +\frac{3}{2}, +\frac{1}{2}\right) + \left(+\frac{1}{2}, -\frac{1}{2}, +\frac{1}{2}\right) + \left(-\frac{1}{2}, +\frac{1}{2}, +\frac{1}{2}\right)\right\}$$

$S_T = \frac{1}{2}$, $S_{12} = 0$:

$$\psi\left(\frac{1}{2}, \frac{1}{2}\right) = \frac{1}{2}\left\{\left(+\frac{3}{2}, -\frac{3}{2}, +\frac{1}{2}\right) - \left(-\frac{3}{2}, +\frac{3}{2}, +\frac{1}{2}\right) - \left(+\frac{1}{2}, -\frac{1}{2}, +\frac{1}{2}\right) + \left(-\frac{1}{2}, +\frac{1}{2}, +\frac{1}{2}\right)\right\}$$